Current Biology 24, 1447–1455, July 7, 2014 ©2014 Elsevier Ltd All rights reserved http://dx.doi.org/10.1016/j.cub.2014.05.031

Article

Perceptual Gap Detection Is Mediated by Gap Termination Responses in Auditory Cortex

Aldis P. Weible,[1] Alexandra K. Moore,[1] Christine Liu,[1] Leah DeBlander,[1] Haiyan Wu,[1] Clifford Kentros,[1,2] and Michael Wehr[1,*]

[1]Institute of Neuroscience, University of Oregon, Eugene, OR 97405, USA

[2]Kavli Institute, 7491 Trondheim, Norway

Summary

Background: Understanding speech in the presence of background noise often becomes increasingly difficult with age. These age-related speech processing deficits reflect impairments in temporal acuity. Gap detection is a model for temporal acuity in speech processing in which a gap inserted in white noise acts as a cue that attenuates subsequent startle responses. Lesion studies have shown that auditory cortex is necessary for the detection of brief gaps, and auditory cortical neurons respond to the end of the gap with a characteristic burst of spikes called the gap termination response (GTR). However, it remains unknown whether and how the GTR plays a causal role in gap detection. We tested this by optogenetically suppressing the activity of somatostatin- or parvalbumin-expressing inhibitory interneurons, or CaMKII-expressing excitatory neurons, in auditory cortex of behaving mice during specific epochs of a gap detection protocol.

Results: Suppressing interneuron activity during the postgap interval enhanced gap detection. Suppressing excitatory cells during this interval attenuated gap detection. Suppressing activity preceding the gap had the opposite behavioral effects, whereas prolonged suppression across both intervals had no effect on gap detection.

Conclusions: In addition to confirming cortical involvement, we demonstrate here for the first time a causal relationship between postgap neural activity and perceptual gap detection. Furthermore, our results suggest that gap detection involves an ongoing comparison of pre- and postgap spiking activity. Finally, we propose a simple yet biologically plausible neural circuit that reproduces each of these neural and behavioral results.

Introduction

Understanding speech in noisy environments, such as a crowded restaurant, often becomes increasingly difficult with age. Age-related speech processing deficits can occur even with completely normal audiometric hearing and are instead associated with temporal processing deficits [1, 2]. In contrast to declines in audiometric hearing, which are associated with the peripheral auditory system [3], age-related temporal processing deficits involve higher-order structures [4–6]. Lesion studies suggest that auditory cortex is essential for temporal acuity [7–9]. However, lesions cannot reveal the contributions of specific cortical circuits or cell types, nor can they reveal any of the dynamic processing by which these circuits mediate temporal processing. Moreover, most neurophysiological studies of temporal processing have been only correlative. As a result, the mechanisms underlying temporal processing in cortex are not well understood.

A well-established measure of temporal processing in both humans and animals is gap detection. In this variant of prepulse inhibition, a silent gap is inserted into continuous background noise. The gap acts as a cue that reduces the startle response evoked by a subsequent loud noise burst. Gaps as brief as 2–4 ms measurably attenuate the startle response in species as diverse as mice [7], zebra finches [10], and humans [11]. Cortical deactivation studies have shown that auditory cortex is necessary for the detection of brief gaps ($\leq$50 ms), but not for long gaps (75–100 ms; [7, 9]). The duration of the briefest detectable gap is referred to as the minimum gap threshold (MGT). Auditory cortical neurons respond to the end of the gap with a characteristic burst of spikes called the gap termination response (GTR). The cortical GTR has an MGT similar to that of behavioral startle attenuation, and both grow with increasing gap durations [7, 9, 12]. The cortical GTR has therefore been proposed as a neural correlate of brief gap detection [12, 13].

Demonstrating a causal link between the cortical GTR and perceptual gap detection requires manipulating the GTR itself. The challenge lies in manipulating neural activity only during the brief interval (50 ms) when the GTR occurs, between the gap termination and the onset of the startle stimulus. Here we used optogenetic suppression to specifically manipulate the GTR. We measured gap detection in transgenic mice expressing archaerhodopsin (Arch; [14]) in one of three different neuronal populations: parvalbumin-expressing (PV) GABAergic interneurons, somatostatin-expressing (SOM) GABAergic interneurons, or CaMKII-expressing pyramidal neurons (PNs). Both PV and SOM interneurons have a predominantly inhibitory role, reducing excitatory PN activity [15–19]. We predicted that suppressing the activity of these inhibitory cells during the postgap interval would increase the GTR and enhance gap detection. Conversely, we predicted that suppressing CaMKII-expressing pyramidal neurons during the same interval would decrease the GTR and reduce gap detection. We also tested the effects of cortical manipulation during other epochs of the task to determine the specificity with which the GTR is responsible for brief gap detection, and how it interacts with activity during other epochs of the task.

We found that suppressing SOM- or PV-expressing inhibitory interneurons (INs) immediately following brief gaps enhanced gap detection. Suppressing CaMKII-expressing excitatory neurons during this period reduced gap detection. This demonstrates for the first time the functional relationship between cortical GTRs and perceptual gap detection. By contrast, suppression limited to the pregap interval elicited the opposite behavioral effects. Prolonged suppression throughout both pre- and postgap intervals had no effect on gap detection. Taken together, these data indicate that gap detection involves a comparison between pre- and postgap neuronal activity. We illustrate this idea with a simple neural

*Correspondence: wehr@uoregon.edu

circuit model that implements such a comparison and reproduces our neural and behavioral results.

Results

We tested the ability of mice to detect gaps of 2, 4, 6, 8, 10, 25, and 50 ms embedded in continuous 80 dB white noise. Gap detection was measured by the attenuation of the startle response evoked by a 100 dB burst of noise, presented 50 ms after the gap. On alternating trials, we suppressed the activity of SOM- or PV-expressing inhibitory interneurons or CaMKII-expressing excitatory PNs during (1) the 50 ms interval between gap termination and startle onset, which includes the GTR ("postgap" suppression); (2) the 940 ms interval preceding gap onset ("pregap" suppression); or (3) the entire 1,000 ms preceding startle onset ("prolonged" suppression both before and after the gap). In separate experiments in anesthetized mice, we determined the optimal coordinates for optical fiber placement (see Figure S2 available online), measured the spread of suppression at different laser intensities (Figure S3), and electrophysiologically verified the efficacy of optogenetic suppression. We also verified in awake mice the electrophysiological effects of suppression directly on the GTR (Figure S4). We used two laser intensities: 300 mW/mm^2, which affected only auditory cortex and provided moderate suppression, and 1,000 mW/mm^2, which provided more robust suppression in auditory cortex but may have affected adjacent cortical and subcortical regions (Figure S3).

Effects of SOM Interneuron Suppression

Auditory cortex is necessary for brief gap detection, and the amplitude of the cortical GTR is correlated with both detection threshold and the degree of startle attenuation [7, 9, 12]. SOM interneurons are found throughout the depth of cortex and therefore could be highly effective in suppressing auditory cortical activity [20–22]. We verified that SOM cells expressed Arch (Figure 1A), that their laminar distribution was consistent with previous reports (Figure 1B; [20–22]), and that suppression of SOM cells significantly increased PN spiking activity (Figure 1C). If a causal link exists between the GTR and gap perception, we hypothesized that suppression of SOM activity during the postgap interval would increase the GTR and result in greater attenuation of the startle reflex. Consistent with this prediction, suppression during the postgap period significantly attenuated startle responses following gaps $\leq$ 25 ms, but not gaps of 50 ms (Figure 1D). In other words, detection was improved for brief gaps. This effect was more pronounced with the higher laser intensity (1,000 mW/mm^2; Figure 1E). The MGT was 4 ms and was not affected by SOM suppression at either intensity. SOM suppression in the 0 ms gap condition had no effect, indicating a specific effect of suppression on gap detection. Moreover, the laser had no effect in Arch-negative SOM littermate controls (Figure 1H).

We next suppressed SOM interneurons during other temporal epochs of the gap detection protocol. Surprisingly, suppressing SOM activity in the pregap period increased startle amplitudes (Figure 1F), indicating a decrease in gap detection. Even more interestingly, when we instead suppressed SOM interneurons uniformly across both the pregap and postgap intervals ("prolonged suppression"), there was no effect on startle responses (Figure 1G). These two results suggest the existence of a dynamic comparison between pregap and postgap spiking activity.

Effects of PV Interneuron Suppression

PV-expressing interneurons also inhibit pyramidal neurons and have distinct neurochemical, morphological, and electrophysiological phenotypes compared to SOM interneurons [22–25]. We therefore expected that, like SOM interneurons, suppressing this population would improve gap detection. Here, too, our expectations were confirmed, although the effect was less robust. We first verified that PV cells expressed Arch (Figure 2A), that their laminar distribution was consistent with previous reports (Figure 2B; [26]), and that suppression of PV cells significantly increased PN spiking activity (Figure 2C). Postgap suppression of PV cells significantly reduced startle amplitudes following gaps $\leq$ 10 ms but had no effect for gaps of 25 ms or 50 ms (Figure 2D). As with the SOM animals, the effect was more robust with the higher laser intensity (1,000 mW/mm^2; Figure 2E). The MGT was reduced from 4 ms to 2 ms at the higher intensity ($df = 179$, $t = 3.83$, $p = 0.0002$) but was unaffected at the lower intensity.

No significant effect was seen with pregap PV suppression, although as with SOM suppression, the trend was in the direction of increased startle amplitudes (Figure 2F). Prolonged PV suppression, in turn, had no effect on gap detection (Figure 2G). Illumination again had no effect in Arch-negative PV littermate controls (Figure 2H).

Finally, to test whether the effects of interneuron suppression were specific to gap detection or more generally affected the gain of startle response circuitry, we measured conventional prepulse inhibition (using white-noise bursts as the prepulses, presented in a silent background). PV and SOM suppression had no effect on prepulse inhibition (Figure S5), indicating that the effects we observed were specific for gap detection.

Effects of CaMKII Pyramidal Neuron Suppression

We verified that CaMKII cells expressed Arch (Figure 3A), that their laminar distribution was consistent with previous reports (Figure 3B; [27]), and that suppression of CaMKII cells significantly reduced PN spiking activity (Figure 3C). Suppressing SOM or PV inhibitory neurons during the postgap interval improved gap detection. We predicted that suppressing pyramidal neurons during this interval would have the opposite effect. Indeed, postgap suppression of CaMKII neurons following gaps $\leq$ 10 ms significantly reduced startle attenuation (i.e., impaired gap detection; Figure 3D). No effects were seen following gaps of 25 ms or 50 ms. The effect was more pronounced with the higher laser intensity (1,000 mW/mm^2; Figure 3E). The MGT of 4 ms was not affected at either intensity. Conversely, suppressing CaMKII neurons during the pregap interval decreased startle amplitudes (Figure 3F), indicating improved gap detection. Prolonged suppression again produced no effect (Figure 3G). Laser illumination had no effect on Arch-negative CaMKII littermate controls (Figure 3H).

A Circuit Model for Gap Detection

We found that increasing or decreasing the activity of pyramidal neurons during either the pregap or postgap periods caused opposing effects on gap detection, whereas prolonged suppression throughout the pre- and postgap period had no effect. This suggests the existence of a process that compares postgap activity to pregap activity. One simple yet biologically plausible mechanism that could perform such a comparison is a circuit that subtracts the recent history

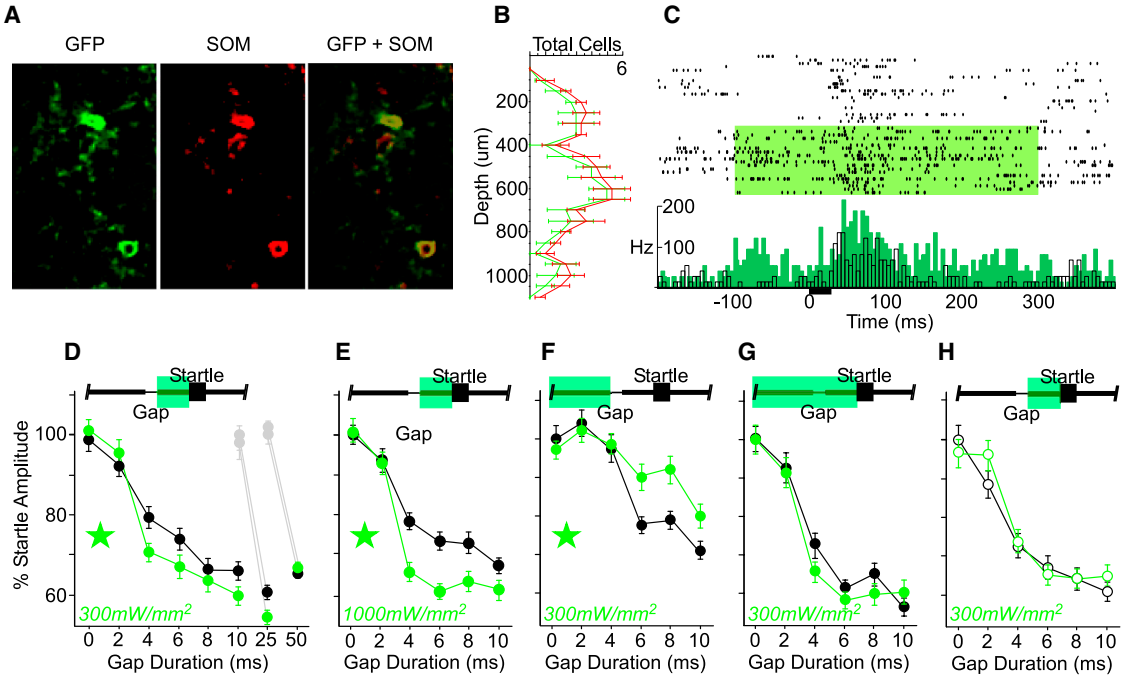

Figure 1. Optogenetic Suppression of SOM Interneurons Enhances Gap Detection

(A) Colocalization of Arch-GFP native fluorescence (GFP) and somatostatin antibody labeling. 84% of somatostatin-positive cells expressed GFP (n = 4 sections, 2 mice).

(B) SOM interneurons were distributed throughout layers 2–6 in auditory cortex. The laminar distribution of GFP-labeled cells matched that of the overall somatostatin-positive population. Error bars show SEM.

(C) To confirm that activating Arch increased spiking activity in PNs, we recorded single-unit and multiunit activity in anesthetized SOM mice. Illustrated is an example multiunit recording from an anesthetized SOM animal. Top: raster plot of responses to a 25 ms white-noise burst (black bar), grouped by "laser off" and "laser on" trials (green shading; 300 mW/mm^2). Bottom: same data, shown as mean firing rate (black, "laser off"; green, "laser on"; 5 ms bins). Suppressing SOM interneurons caused a significant increase in driven (0 to 100 ms) and spontaneous (−100 to 0 ms) spiking activity. Efficacy was verified in four mice. Suppressing SOM interneurons (300 mW/mm^2) significantly increased sound-evoked spiking activity for 9 of 23 recordings (39%), 4 of which also showed a significant increase in spontaneous activity. Interestingly, most of these effects were seen in the subgranular layers: 75% of multiunit sites deeper than 500 μm showed significant effects of laser illumination.

(D–H) Gap detection behavior. The green bar at the top of each panel indicates the laser duration relative to gap and startle stimuli; green stars indicate significance by ANOVA; error bars show SEM.

(D) Postgap suppression, low intensity. Suppression of SOM interneurons specifically during the postgap interval significantly attenuated startle responses (indicating enhanced gap detection) following gaps $\leq$ 10 ms (interaction $F_{5,1430} = 2.22$, $p = 0.049$; 3 mice, 12 sessions) and 25 ms (df = 718, t = 2.6, $p = 0.009$; 3 mice, 10 sessions), but not 50 ms (4 mice, 12 sessions). Gray symbols correspond to the 0 ms gap presentations during separate assessment of 25 or 50 ms gap detection.

(E) Postgap suppression, high intensity. Increasing the laser intensity to 1,000 mW/mm^2 further attenuated the startle following gaps $\leq$ 10 ms (main effect $F_{1,206} = 14.98$, $p = 0.0001$; interaction $F_{5,1030} = 3.338$, $p = 0.006$; 2 mice, 10 sessions).

(F) Pregap suppression, low intensity. Suppression restricted to the pregap interval, beginning 1,000 ms prior to startle onset, enhanced startle responses to gaps $\leq$ 10 ms (main effect $F_{1,234} = 4.71$, $p = 0.031$; interaction $F_{5,1170} = 3.37$, $p = 0.005$; 4 mice, 10 sessions).

(G) Prolonged suppression, low intensity. Prolonged suppression, beginning 1,000 ms prior to startle onset and continuing through the postgap interval, had no effect on gap detection (3 mice, 12 sessions).

(H) Gap detection was unaffected by the laser in Arch-negative SOM littermate controls (open circles; 3 mice, 10 sessions).

of PNs. Inhibitory interneurons would be well suited to this operation, but other forms of adaptation (such as synaptic depression) could perform similar operations. To test whether such a mechanism could account for our results, we constructed a simple neural model that is schematized in Figure 4A (inset). Sound input is passed sequentially through two PNs; at each step, an inhibitory interneuron (shown in red) computes a running average of its recent input and provides subtractive inhibition. This circuit motif produced GTRs that depended on gap duration (Figure 4A, black lines). The final PN output proportionally reduced startle responses, so that the model simulated gap detection with the same units (% startle amplitude) as our behavioral data. The model accurately captured how startle amplitude is progressively decreased by longer gaps (Figure 4B, black points).

We simulated optogenetic suppression of PNs as a subtractive term indicated by green shaded regions in Figures 4A, 4C, and 4E. Postgap suppression reduced the GTR (Figure 4A, green lines), producing a gap detection deficit (i.e., increased startle amplitude; green symbols in Figure 4B). This qualitatively matches the gap detection deficit that was caused by suppressing PNs in mice (Figures 3D and 3E). When we instead applied PN suppression to the pregap period, the GTR was actually enhanced, as shown by the green lines in Figure 4C. This enhancement can be thought of as a type of rebound from inhibition. When pregap PN activity is optogenetically reduced, the amount of inhibition is also reduced. This inhibition remains reduced during the postgap period, because the weighted running average continues to be affected by pregap PN activity. This reduced inhibition increases postgap PN

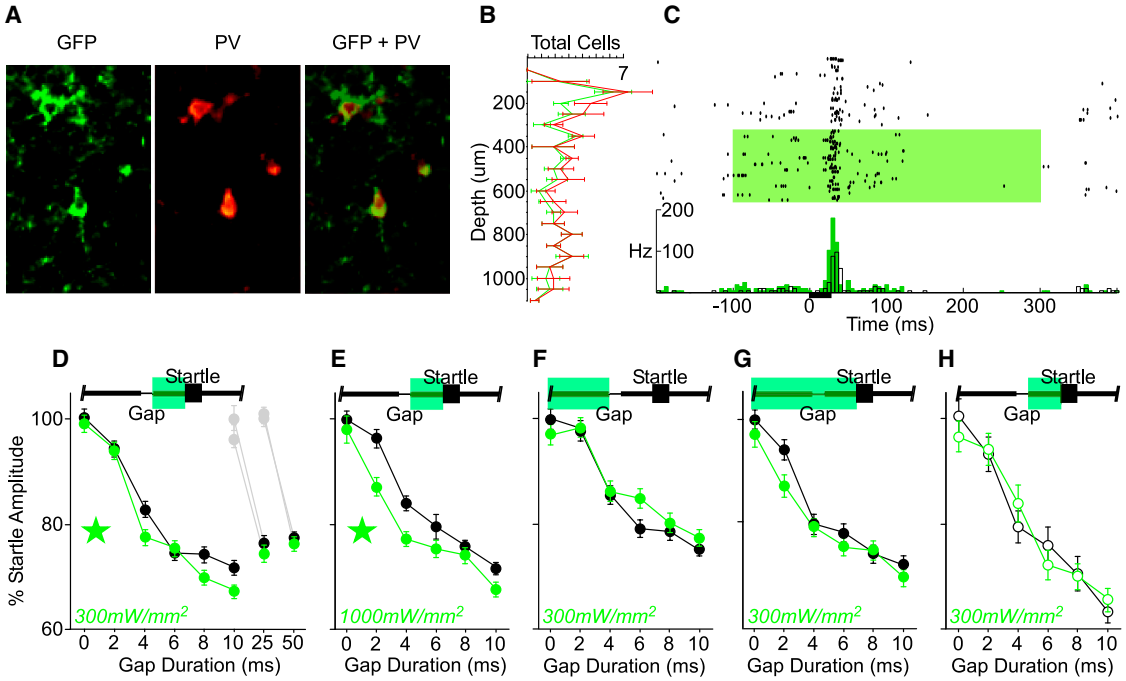

Figure 2. Optogenetic Suppression of PV Interneurons Enhances Gap Detection

(A) Colocalization of Arch-GFP native fluorescence and parvalbumin antibody labeling. 82% of parvalbumin-positive cells expressed GFP (n = 4 sections, 2 mice).

(B) PV interneurons were distributed throughout layers 2–6 in auditory cortex. The laminar distribution of GFP-labeled cells matched that of the overall parvalbumin-positive population. Error bars show SEM.

(C) To confirm that activating Arch increased spiking activity in PNs, we recorded single-unit activity in anesthetized PV mice. Illustrated is an example single-unit recording from an anesthetized PV animal. Top: raster plot of responses to a 25 ms white-noise burst (black bar), grouped by "laser off" and "laser on" trials (green shading; 300 mW/mm^2). Bottom: same data, shown as mean firing rate (black, "laser off"; green, "laser on"; 5 ms bins). Suppressing PV interneurons caused a significant increase in driven (0 to 100 ms) and spontaneous (−100 to 0 ms) spiking activity. Efficacy was verified in four mice. Suppressing PV interneurons (300 mW/mm^2) significantly increased sound-evoked spiking for 24 of 28 recordings (85%), 12 of which also showed a significant increase in spontaneous activity.

(D–H) Gap detection behavior. The green bar at the top of each panel indicates the laser duration relative to gap and startle stimuli; green stars indicate significance by ANOVA; error bars show SEM.

(D) Postgap suppression, low intensity. Suppression of PV interneurons specifically during the postgap interval significantly attenuated startles following gaps $\leq$ 10 ms (main effect $F_{1,403} = 4.2$, $p = 0.04$; 4 mice, 18 sessions), but not 25 or 50 ms (2 mice, 11 sessions; 2 mice, 10 sessions). Gray symbols correspond to the 0 ms gap presentations during separate assessment of 25 or 50 ms gap detection.

(E) Postgap suppression, high intensity. Increasing the laser intensity to 1,000 mW/mm^2 further attenuated the startle following gaps $\leq$ 10 ms (main effect $F_{1,358} = 15.591$, $p < 0.0001$; 3 mice, 15 sessions).

(F) Pregap suppression, low intensity. Suppression restricted to the pregap interval did not significantly impact detection of gaps $\leq$ 10 ms, though reduced attenuation was evident at several gap durations (2 mice, 16 sessions).

(G) Prolonged suppression, low intensity. Prolonged suppression did not significantly influence detection of gaps $\leq$ 10 ms (4 mice, 12 sessions).

(H) Gap detection was unaffected by the laser in Arch-negative PV littermate controls (open circles; 2 mice, 9 sessions).

activity and enhances gap detection performance (Figure 4D), which matches the results in mice (Figure 3F). Finally, we simulated prolonged suppression throughout the pre- and postgap periods (Figure 4E). Here, suppression had no effect on PN responses or simulated gap detection behavior (Figure 4F), similar to what we observed in mice (Figure 3G). This makes sense, because the gap detection circuit motif is sensitive only to changes in activity. Prolonged optogenetic suppression merely adds a constant offset to activity in the circuit, which is removed by the inhibitory interneurons, producing no net effect. This pattern of results was qualitatively unchanged across a wide range of model parameters, and even different model architectures (see Supplemental Experimental Procedures), as long as the circuit included an inhibitory interneuron sensitive to recent history. These results suggest that this simple and biologically plausible circuit motif could explain the opposing effects caused by suppressing PNs during different task epochs.

The same circuit model also accounted for the effects of suppressing inhibitory interneurons (Figure 5). Here, we simulated suppression of SOM or PV cells by applying a subtractive term to the second interneuron (red cell in Figure 5A, inset). This produced the opposite pattern of results as suppressing PNs: suppressing INs during the postgap period enhanced the PN GTR (Figure 5A), thereby enhancing gap detection (i.e., reducing startle amplitudes; Figure 5B). This makes sense, because removing inhibition during the postgap interval should directly increase the strength of the GTR. Suppressing INs during the pregap period decreased the PN GTR (Figure 5C) and thereby decreased gap detection (Figure 5D). Intuitively, this occurs because suppressing INs causes elevated PN activity during the pregap period, which in turn leads to excess inhibition in the postgap period after INs are released from suppression. Prolonged suppression of INs during the pre- and postgap periods produced no net

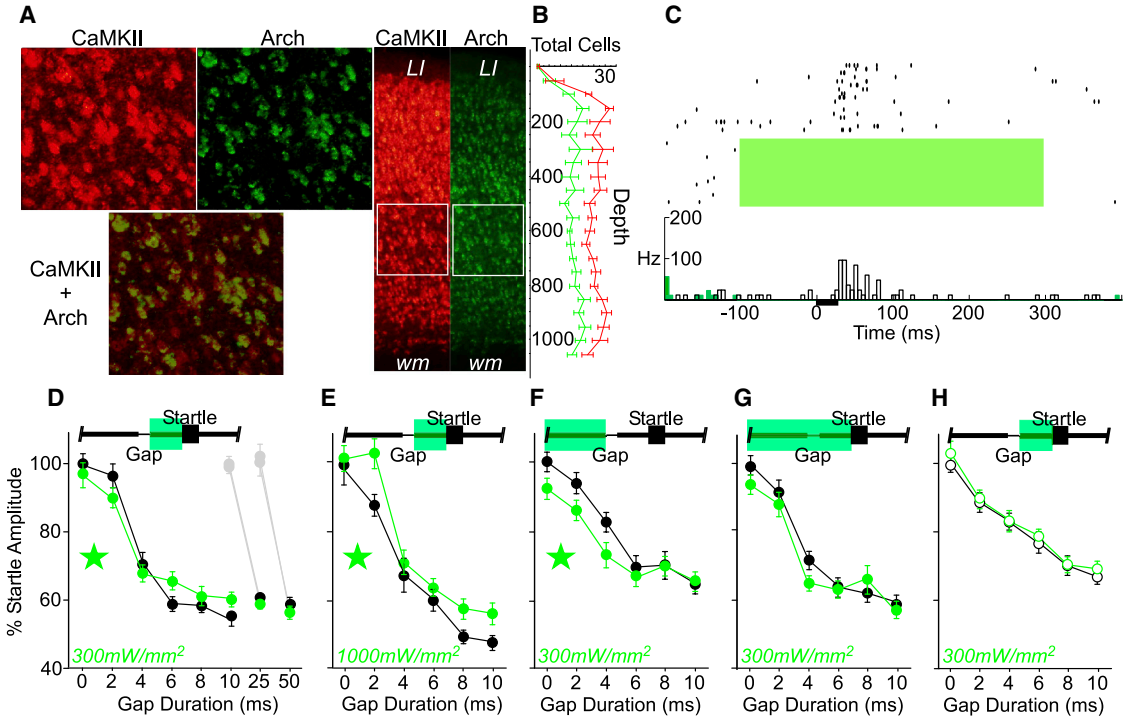

Figure 3. Optogenetic Suppression of CaMKII-Expressing Pyramidal Neurons Reduces Gap Detection

(A) Dual fluorescence in situ hybridization showing colocalization of CaMKII and Arch. White boxes show the laminar position of the high-magnification photos (LI, layer I; wm, white matter). 64% of CaMKII-positive neurons were positive for Arch (n = 5 sections, 5 mice).

(B) Arch expression was distributed across cortical layers (data averaged across n = 5 sections from n = 5 mice). Error bars show SEM.

(C) To confirm that Arch suppresses spiking activity in PNs, we recorded single-unit and multiunit activity in anesthetized CaMKII mice. Illustrated is an example multiunit recording from an anesthetized CaMKII animal. Top: raster plot of responses to a 25 ms white-noise burst (black bar), grouped by "laser off" and "laser on" trials (green shading; 300 mW/mm^2). Bottom: same data, shown as mean firing rate (black, "laser off"; green, "laser on"; 5 ms bins). Illumination significantly suppressed driven (0 to 100 ms) and spontaneous (−100 to 0 ms) spiking activity (note the complete absence of spikes during suppression). Efficacy was verified in five mice. Illumination (300 mW/mm^2) significantly suppressed sound-evoked spiking activity in 16 of 22 recordings (72%) and suppressed spontaneous activity in 20 of 22 recordings (90%).

(D–H) Gap detection behavior. The green bar at the top of panels indicates the laser duration relative to gap and startle stimuli; green stars indicate significance by ANOVA; error bars are SEM.

(D) Postgap suppression, low intensity. Suppressing pyramidal neurons during the postgap interval significantly increased startle responses following gaps $\leq$ 10 ms (interaction $F_{5,1550} = 2.75$, p = 0.018; 3 mice, 13 sessions), but not 25 or 50 ms (2 mice, 7 sessions; 3 mice, 9 sessions). Gray symbols correspond to the 0 ms gap presentations during separate assessment of 25 or 50 ms gap detection.

(E) Postgap suppression, high intensity. Increasing the laser intensity to 1,000 mW/mm^2 robustly increased the startle enhancement following gaps $\leq$ 10 ms (main effect $F_{1,382} = 9.51$, p = 0.002; 3 mice, 16 sessions).

(F) Pregap suppression, low intensity. Suppression restricted to the pregap interval significantly reduced startles following gaps $\leq$ 10 ms (main effect $F_{1,238} = 5.107$, p = 0.025; 2 mice, 10 sessions).

(G) Prolonged suppression, low intensity. Prolonged suppression did not significantly influence detection of gaps $\leq$ 10 ms (4 mice, 10 sessions).

(H) Gap detection was unaffected by the laser in Arch-negative CaMKII littermate controls (open circles; 2 mice, 8 sessions).

effect on PN activity or behavioral output, for the same reason that prolonged suppression of PNs has no effect in the change-detection circuit. If INs mediate the comparison that subserves gap detection, as we propose, why then does suppressing them not eliminate gap detection? Although complete suppression (as with a lesion) would indeed eliminate gap detection according to our model, our partial optogenetic suppression instead affects the gain of cortical responses while still allowing residual IN function to mediate the subtractive comparison. Alternatively, the comparison could be mediated by another form of adaptation, such as synaptic depression.

Discussion

Gap detection is a measure of auditory temporal acuity and a model for speech perception. Detection of brief gaps, which are analogous to the dips in spectrotemporal energy occurring within and between phonemes in speech, is cortically dependent, although the mechanisms underlying this process have remained unclear. Here we provide evidence suggesting a causal link between the cortical GTR and perceptual gap detection. By optogenetically manipulating neural activity specifically during the interval containing the GTR, we altered the gap-induced attenuation of startle responses. Suppressing cortical pyramidal neuron activity reduced perceptual gap detection, whereas suppressing cortical PV or SOM inhibitory interneurons enhanced gap detection. Suppression had no effect on prepulse inhibition, indicating that the effects we observed were specific for gap detection. In general, manipulating cortical activity affected the degree of startle attenuation without affecting the MGT, suggesting that cortical manipulation affects gap salience rather than temporal acuity (although PV suppression at higher intensities did reduce the MGT).

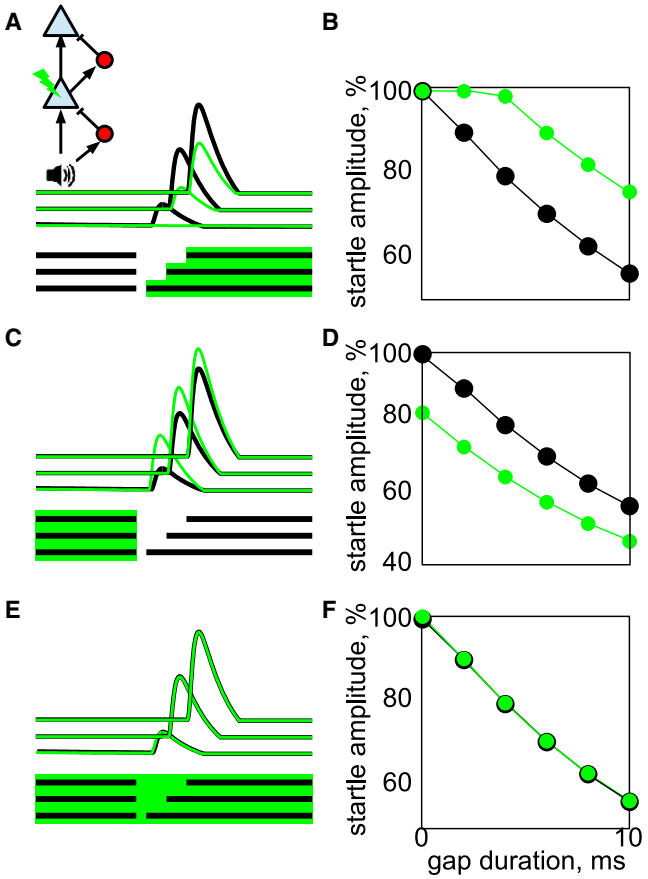

Figure 4. A Simple Circuit Model Reproduces the Neural and Behavioral Effects of Optogenetically Suppressing PNs

(A) Inset: in the circuit model, sound input is passed through two layers, each consisting of a PN (pyramidal neuron, light blue triangle) and an IN (interneuron, red circle). The IN computes an exponentially weighted running average of its input and produces a subtractive output to its target. Optogenetic suppression of the lower PN is indicated by a lightning bolt symbol and was simulated by a subtractive term. Gap stimuli are indicated by horizontal black bars; gaps of 2, 6, and 10 ms are shown. Black lines show the responses of the upper PN to each gap stimulus; green lines show the same responses when simulated optogenetic suppression was applied during the time indicated by the green shaded region below. Note that postgap suppression reduced the PN gap termination response.

(B) We modeled behavioral gap detection readout (black circles) by reducing startle amplitude proportional to the amplitude of the PN gap termination response. Green circles show gap detection during suppression of the postgap period as indicated in (A). Compare to Figures 3D and 3E.

(C and D) Suppression applied during the pregap period had the opposite effect of increasing PN gap termination responses (C) and enhancing gap detection (D).

(E and F) Prolonged suppression applied during the entire pre- and postgap period had no effect on PN responses (E) or gap detection performance (F).

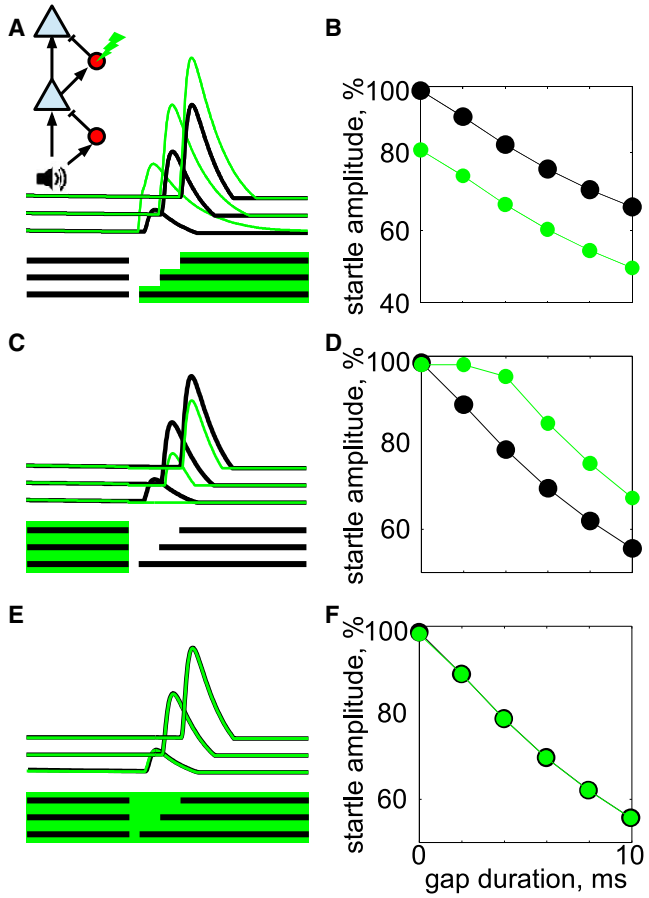

Figure 5. A Simple Circuit Model Reproduces the Neural and Behavior Effects of Optogenetically Suppressing Inhibitory INs

(A and B) Inset: same circuit model as in Figure 4A, but optogenetic suppression was applied to the upper cortical interneuron (red circle with lightning bolt symbol). Format is as in Figure 4. Postgap suppression of the IN increased the PN gap termination response (A) and enhanced gap detection performance (B). Compare to Figures 1D and 1E.

(C and D) Suppression applied during the pregap period had the opposite effect of decreasing PN gap termination responses (C) and impairing gap detection (D).

(E and F) Prolonged suppression applied during the entire pre- and postgap period had no effect on PN responses (E) or gap detection performance (F).

Furthermore, by suppressing activity before the gap, directly after the gap, or both, we demonstrate that gap perception involves a comparison between pre- and postgap neuronal activity. These results are summarized in Table 1. Finally, we show that a simple yet biologically plausible neural model implementing such a comparison can reproduce these results. These findings illustrate how shifts in the balance of cortical activity directly impact auditory processes that may be involved in speech perception.

Importantly, our experimental design rules out the possibility of nonspecific suppression effects, or that laser illumination acted as a visual cue. Because of the temporal precision with which we could suppress neural activity, we were able to show distinct and opposing effects of neural suppression before and after the gap, as well as the null effect of suppressing activity across both intervals. Furthermore, we saw these effects at 300 mW/mm^2, for which suppression was restricted to auditory cortex. This spatial and temporal specificity of suppression supports a causal role of the GTR in auditory cortex for gap detection. We can rule out the possibility that the laser acted as a visual cue by two observations. First, we saw no effect of light delivery in control animals (littermates not expressing Arch). Second, there was no effect of laser for a gap of 0 ms (i.e., no gap). Suppression only affected behavior when coupled with the presentation of a gap, and therefore did not modify startle responses in and of itself. The effect of suppression was modest (7%–10% at 300 mW/mm^2; 10%–16% at 1,000 mW/mm^2) but was within the range reported for other paradigms that measure effects on startle response (e.g., [28]).

Table 1. Behavioral Summary by Suppression Protocol

	Postgap Suppression	Pregap Suppression	Prolonged Suppression
	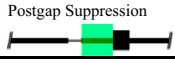	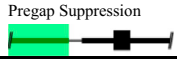	
SOM	decreases startle	increases startle	no effect
PV	decreases startle	increases startle*	no effect
CaMKII	increases startle	decreases startle	no effect

*Nonsignificant trend.

In auditory cortex, transient onset responses can distinguish between similar sounds such as phonemes [29–33]. Onset responses following gaps in noise (i.e., GTRs) increase with gap duration [12]. This scaling of response amplitude may provide one of the critical cues for accurate perception of phonemes and other sounds. Our results support this idea. By increasing or decreasing the GTR, we evoked startle responses characteristic of shorter or longer gaps, respectively. For example, startles elicited by a 4 ms gap during SOM suppression were comparable to startles elicited by an 8 ms gap in control conditions. These results not only indicate a change in gap perception but also demonstrate how the GTR encodes the temporal properties of auditory events. This has important implications for age-related hearing loss, since both PV and SOM inhibition decline with age [34–37]. The loss of inhibition with age not only may generally disrupt temporal processing but may specifically shift perception (such that an 8 ms gap, for example, is perceived as a 4 ms gap). This could cause misclassification of phonemes that are distinguished by parametric variation in temporal structure, such as voice-onset time. Since both onset and offset responses in auditory cortex are frequency tuned [38], it will be interesting to see whether the results that we obtained using gaps in broadband noise also generalize to tones of a specific frequency.

Although our data support a role for auditory cortex in brief gap detection, the effects we observed for PN suppression during the postgap interval (Figure 3D) were modest compared with those obtained using conventional lesion techniques [7–9]. The most likely explanation for this is that our CaMKII-Arch optogenetic system suppressed spiking by between 8%–73% (Figure S3), depending on the distance from the fiber tip, at a laser intensity of 300 mW/mm^2. Therefore, the GTR was not completely silenced in our experiments but rather was reduced in amplitude, resulting in incomplete disruption of gap detection. The greater neural and behavioral suppression seen with 1,000 mW/mm^2 (Figures 3E and S3B) supports this explanation. Lesion and inactivation studies have shown that auditory cortex is necessary for detection of brief ($\leq$50 ms) gaps, but not longer gaps, indicating that noncortical brain regions can mediate longer gap detection [7–9]. By demonstrating that our manipulation affected responses only to brief gaps ($\leq$25 ms), but not longer gaps (50 ms), our data confirm cortical involvement in processing these brief events.

How might auditory cortex mediate these effects on gap detection? Startle responses are mediated by a brainstem circuit in which the cochlear nucleus projects to motor neurons via the nucleus reticularis pontis caudalis (PnC; [39]). Prepulse inhibition, such as that involved with our gap detection task, is thought to act via a circuit from the inferior colliculus (IC) to the superior colliculus (SC) to the cholinergic pedunculopontine tegmental area (PPTg), which suppresses premotor activity in the PnC [40]. Layer 5 neurons in auditory cortex project to IC, SC, and the PPTg [40], and these corticofugal projections would therefore be well suited to mediating cortical effects on gap detection. One might ask why there should be a role for auditory cortex in gap detection, given that IC neurons also have GTRs and are directly involved in the prepulse inhibition circuit. We speculate that auditory cortex may provide the ability to associate gaps or other temporally structured sounds (such as phonemes) with meaning, and that associative learning in auditory cortex may be able to impact behavioral output by means of its corticofugal projections to IC, SC, PPTg, and related structures.

One of the unexpected findings of our study was the evidence of active comparison of pre- and postgap activity in gap detection. It seems likely that this is mediated by some form of adaptation, which strongly shapes cortical responses to auditory events [41–44]. We illustrated how this could work using a simple neural circuit model in which the recent history of pyramidal neurons is subtracted by inhibitory neurons, although other forms of adaptation (such as synaptic depression) could also perform similar operations. This circuit motif qualitatively reproduced both the basic properties of gap detection and the opposing effects of our optogenetic manipulations of the circuit. This qualitative agreement suggests that gap detection indeed involves a comparison mechanism, but it should be noted that there are some quantitative differences between behavioral and model performance (e.g., between Figures 1D–1E and 5B), which suggests that additional mechanisms must be at play. While cortical circuits are undoubtedly more complex than our model, our results provide a plausible biological mechanism for performing a comparison of spiking activity between pre- and postgap periods. The model also makes testable predictions about the gap response properties of pyramidal and inhibitory neurons at different positions in the circuit. It will be of great interest to test these predictions by recording from these cell types in auditory cortex during optogenetic manipulation of gap detection behavior.

We found that reducing inhibition led to an increase in PN GTR amplitude (Figures 1C and 2C), which improved gap detection (Figures 1D, 1E, 2D, and 2E). However, it is still unclear whether the critical effect of reducing inhibition is to increase PN firing rate (i.e., a gain change), to alter the temporal structure of PN responses, or both. In light of the known roles of interneurons in controlling the timing of PN spiking activity [24, 44, 45], it will be interesting to examine how INs shape the temporal dynamics of PN gap responses and how perceptual gap detection depends on that temporal structure.

Experimental Procedures

Animals

All procedures were performed in strict accordance with National Institutes of Health guidelines, as approved by the University of Oregon Institutional Animal Care and Use Committee. See Supplemental Experimental Procedures for detailed surgical procedures.

We measured gap detection behavior in heterozygous offspring (both males and females) of crosses between a cre-dependent Arch line, CAG-Arch-eGFP, and two interneuron lines, Pvalb-IRES-Cre ("PV," n = 5) and SOM-IRES-Cre ("SOM," n = 9). We also measured behavior in mice expressing Arch in pyramidal neurons by crossing a CaMKII-tTA line ("CaMKII," n = 6) to a tTA-dependent Arch line, which we report here for the first time. The generation of the line is described in Supplemental Experimental Procedures ("tetO-ArchT2 Generation"). Arch-negative littermates were used as behavioral controls (PV, n = 2; SOM, n = 3; CaMKII, n = 2). Data were collected from a total of 70 mice, including those used in additional electrophysiological and anatomical expression experiments detailed below and in Supplemental Information. Mean ± SE age was 10 ± 0.3 weeks,

well under the age at which C57BL/6J mice become susceptible to age-related hearing loss [46].

Behavioral Experiments

Fiber Implantation

All mice assessed for gap detection were chronically implanted with a pair of 200 μm optic fibers bilaterally targeting primary auditory cortex using coordinates derived from cortical mapping experiments (see Supplemental Information sections "Fiber Implantation" and "Fiber Coordinate Mapping" and Figure S2 for details).

Data Acquisition and Stimuli

All behavioral data were collected in a sound-attenuating chamber. Sounds were delivered from a free-field speaker facing the animal's right ear. Mice were loosely restrained in a plastic tube with a flat base. To measure startle responses, movement signals from a piezo transducer beneath the tube were amplified 200× and digitized at 10 kHz.

White noise served as both the continuous background (80 dB sound pressure level [SPL]) and startle stimulus (25 ms burst, 100 dB SPL). Startle stimuli were separated by a random intertrial interval of 15 ± 5 s. Gaps in the continuous background noise preceded the startle stimulus, separated by a 50 ms interstimulus interval. Gap detection was assessed for gaps of 0, 2, 4, 6, 8, 10, 25, and 50 ms. Optogenetic suppression of neural activity was applied on alternating trials.

We used three different optogenetic suppression protocols. "Postgap" suppression targeted the interval between gap offset and startle stimulus onset (see Figure 1D). "Pregap" suppression began 1,000 ms prior to startle onset and terminated with gap onset (see Figure 1F). "Prolonged" suppression began 1,000 ms prior to, and terminated with, startle onset, resulting in suppression during both "pregap" and "postgap" intervals (see Figure 1G). The light intensity was 300 mW/mm^2 at the fiber tip (i.e., 9.4 mW of total power through each 200 μm fiber), except where use of the alternative higher intensity of 1,000 mW/mm^2 is indicated (31.4 mW total power).

Analysis

We quantified startle amplitudes by integrating the rectified piezo signal within a 100 ms window following startle onset. Startle amplitudes were normalized within sessions to the mean laser "off" 0 ms gap startle amplitude. Our goal in these experiments was to ascertain whether the suppression of neural activity altered gap attenuation of startle responses. Therefore, only data from sessions with a significant (paired t test, $p < 0.05$) attenuation of startle responses between the 0 ms and the longest "laser off" gaps (10, 25, or 50 ms) were included in the group analyses. Data were collected from multiple sessions across days for each mouse. All comparisons were performed using data from individual trials. Repeated-measures ANOVAs were performed to identify group differences and interactions by gap duration. t tests were performed to assess differences in startle amplitude both between and within gaps. A Bonferroni correction for multiple comparisons was applied for MGT tests, resulting in a minimum significance threshold of $p < 0.01$. MGTs were determined by comparing gaps of 2–10 ms with 0 ms gap presentations separately for "laser on" and "laser off" trials and were defined as the shortest gap duration eliciting a significant reduction in startle amplitude. Note that gaps below the MGT were unaffected by suppression, whereas detection of gaps longer than the MGT was typically affected by suppression. A significant effect of suppression can therefore be indicated by either an ANOVA interaction or a main effect. Startle response amplitudes were not normally distributed (Lilliefors test), but we note that the ANOVA is very robust to deviations from normality [47], and also that our pattern of results was very similar when we used nonparametric tests (see Table S1).

Electrophysiological Experiments

We performed four types of electrophysiological experiments. First, we determined the optimal fiber coordinates for delivering light to the auditory cortex of C57BL/6 mice (see Supplemental Results section "Fiber Coordinate Mapping" and Figure S2). Second, we confirmed that Arch activation had the expected effect on neural activity in auditory cortex in the three lines used in the behavioral experiments (see Supplemental Experimental Procedures section "Electrophysiological Verification"). Third, we determined the working range of light power for suppressing activity in auditory cortex, using optical fibers implanted as in our behavioral animals (see Supplemental Results section "Light Intensity Mapping" and Figure S3). Fourth, we demonstrated that optogenetic suppression of neural activity significantly affects the amplitude of the GTR (see Supplemental Results section "GTR Manipulation" and Figure S4).

Circuit Model

We implemented a simple circuit model that qualitatively captured the structure of our results. The model (Figure 4A, inset) consisted of a sound envelope, which served as input to a pyramidal (excitatory) neuron (PN) and an inhibitory interneuron (IN). The inhibitory neuron integrated its input with an exponentially weighted time window. The PN integrated the sound input and subtractive inhibition [41]. The PN output then served as input to a second PN and IN pair, identical to the first. Behavioral performance depended on the output of the second PN. We modeled optogenetic suppression as a subtractive term applied to either the first PN (Figure 4A, inset) or the second IN (Figure 5A, inset). For full details of the model, see Supplemental Experimental Procedures section "Circuit Model."

Histology

All fiber placements were verified postmortem. Brains were fixed in 4% paraformaldehyde and then sectioned at 50 μm. The presence of eGFP fluorescence and the appropriate location of optic fiber tracks were both confirmed.

We assessed the specificity of Arch expression using the colocalization of native GFP fluorescence and antibody-labeled inhibitory markers (PV, SOM) or, for the CaMKIIa cross, the colocalization of ArchT2 mRNA and CaMKIIa mRNA, visualized by in situ hybridization. All tissue processing and quantification procedures are described in Supplemental Experimental Procedures section "Histological Procedures."

Supplemental Information

Supplemental Information includes six figures, one table, Supplemental Results, and Supplemental Experimental Procedures and can be found with this article online at http://dx.doi.org/10.1016/j.cub.2014.05.031.

Author Contributions

A.P.W. designed and performed experiments, performed analysis, and wrote the manuscript. A.K.M. performed experiments and analysis. C.L. performed experiments and histology. L.D. generated the CaMKII line. H.W. performed in situ hybridizations. C.K. designed the CaMKII line. M.W. designed experiments, performed analysis and modeling, and wrote the manuscript.

Acknowledgments

We would like to thank Jennifer Linden for fruitful discussions. This work was supported by the NIH (1R01DC011379).

Received: January 13, 2014
Revised: May 2, 2014
Accepted: May 14, 2014
Published: June 26, 2014

References

1. Helfer, K.S., and Vargo, M. (2009). Speech recognition and temporal processing in middle-aged women. J. Am. Acad. Audiol. *20*, 264–271.
2. Ben-David, B.M., Chambers, C.G., Daneman, M., Pichora-Fuller, M.K., Reingold, E.M., and Schneider, B.A. (2011). Effects of aging and noise on real-time spoken word recognition: evidence from eye movements. J. Speech Lang. Hear. Res. *54*, 243–262.
3. Ohlemiller, K.K. (2004). Age-related hearing loss: the status of Schuknecht's typology. Curr. Opin. Otolaryngol. Head Neck Surg. *12*, 439–443.
4. Harris, K.C., Wilson, S., Eckert, M.A., and Dubno, J.R. (2012). Human evoked cortical activity to silent gaps in noise: effects of age, attention, and cortical processing speed. Ear Hear. *33*, 330–339.
5. Suta, D., Rybalko, N., Pelánová, J., Popelář, J., and Syka, J. (2011). Age-related changes in auditory temporal processing in the rat. Exp. Gerontol. *46*, 739–746.
6. Walton, J.P., Barsz, K., and Wilson, W.W. (2008). Sensorineural hearing loss and neural correlates of temporal acuity in the inferior colliculus of the C57BL/6 mouse. J. Assoc. Res. Otolaryngol. *9*, 90–101.
7. Ison, J.R., O'Connor, K., Bowen, G.P., and Bocirnea, A. (1991). Temporal resolution of gaps in noise by the rat is lost with functional decortication. Behav. Neurosci. *105*, 33–40.

8. Syka, J., Rybalko, N., Mazelová, J., and Druga, R. (2002). Gap detection threshold in the rat before and after auditory cortex ablation. Hear. Res. *172*, 151–159.
9. Threlkeld, S.W., Penley, S.C., Rosen, G.D., and Fitch, R.H. (2008). Detection of silent gaps in white noise following cortical deactivation in rats. Neuroreport *19*, 893–898.
10. Okanoya, K., and Dooling, R.J. (1990). Detection of gaps in noise by budgerigars (Melopsittacus undulatus) and zebra finches (Poephila guttata). Hear. Res. *50*, 185–192.
11. Plomp, R. (1964). The rate of decay of auditory sensation. J. Acoust. Soc. Am. *36*, 277–282.
12. Recanzone, G.H., Engle, J.R., and Juarez-Salinas, D.L. (2011). Spatial and temporal processing of single auditory cortical neurons and populations of neurons in the macaque monkey. Hear. Res. *271*, 115–122.
13. Eggermont, J.J. (1999). The magnitude and phase of temporal modulation transfer functions in cat auditory cortex. J. Neurosci. *19*, 2780–2788.
14. Boyden, E.S., Zhang, F., Bamberg, E., Nagel, G., and Deisseroth, K. (2005). Millisecond-timescale, genetically targeted optical control of neural activity. Nat. Neurosci. *8*, 1263–1268.
15. Berger, T.K., Silberberg, G., Perin, R., and Markram, H. (2010). Brief bursts self-inhibit and correlate the pyramidal network. PLoS Biol. *8*, e1000473.
16. Cruikshank, S.J., Lewis, T.J., and Connors, B.W. (2007). Synaptic basis for intense thalamocortical activation of feedforward inhibitory cells in neocortex. Nat. Neurosci. *10*, 462–468.
17. Fino, E., and Yuste, R. (2011). Dense inhibitory connectivity in neocortex. Neuron *69*, 1188–1203.
18. Silberberg, G., and Markram, H. (2007). Disynaptic inhibition between neocortical pyramidal cells mediated by Martinotti cells. Neuron *53*, 735–746.
19. Sohal, V.S., Zhang, F., Yizhar, O., and Deisseroth, K. (2009). Parvalbumin neurons and gamma rhythms enhance cortical circuit performance. Nature *459*, 698–702.
20. Ma, Y., Hu, H., Berrebi, A.S., Mathers, P.H., and Agmon, A. (2006). Distinct subtypes of somatostatin-containing neocortical interneurons revealed in transgenic mice. J. Neurosci. *26*, 5069–5082.
21. Adesnik, H., Bruns, W., Taniguchi, H., Huang, Z.J., and Scanziani, M. (2012). A neural circuit for spatial summation in visual cortex. Nature *490*, 226–231.
22. Wang, Y., Toledo-Rodriguez, M., Gupta, A., Wu, C., Silberberg, G., Luo, J., and Markram, H. (2004). Anatomical, physiological and molecular properties of Martinotti cells in the somatosensory cortex of the juvenile rat. J. Physiol. *561*, 65–90.
23. Kawaguchi, Y., and Shindou, T. (1998). Noradrenergic excitation and inhibition of GABAergic cell types in rat frontal cortex. J. Neurosci. *18*, 6963–6976.
24. Moore, A.K., and Wehr, M. (2013). Parvalbumin-expressing inhibitory interneurons in auditory cortex are well-tuned for frequency. J. Neurosci. *33*, 13713–13723.
25. Li, L.Y., Xiong, X.R., Ibrahim, L.A., Yuan, W., Tao, H.W., and Zhang, L.I. (2014). Differential receptive field properties of parvalbumin and somatostatin inhibitory neurons in mouse auditory cortex. Cereb. Cortex. Published online January 14, 2014. http://dx.doi.org/10.1093/cercor/bht417.
26. Yuan, K., Shih, J.Y., Winer, J.A., and Schreiner, C.E. (2011). Functional networks of parvalbumin-immunoreactive neurons in cat auditory cortex. J. Neurosci. *31*, 13333–13342.
27. Ochiishi, T., Terashima, T., and Yamauchi, T. (1994). Specific distribution of Ca2+/calmodulin-dependent protein kinase II alpha and beta isoforms in some structures of the rat forebrain. Brain Res. *659*, 179–193.
28. Berg, W.K., and Davis, M. (1985). Associative learning modifies startle reflexes at the lateral lemniscus. Behav. Neurosci. *99*, 191–199.
29. Brugge, J.F., and Merzenich, M.M. (1973). Responses of neurons in auditory cortex of the macaque monkey to monaural and binaural stimulation. J. Neurophysiol. *36*, 1138–1158.
30. DeWeese, M.R., Wehr, M., and Zador, A.M. (2003). Binary spiking in auditory cortex. J. Neurosci. *23*, 7940–7949.
31. Eggermont, J.J. (1999). Neural correlates of gap detection in three auditory cortical fields in the Cat. J. Neurophysiol. *81*, 2570–2581.
32. Phillips, D.P., Hall, S.E., and Boehnke, S.E. (2002). Central auditory onset responses, and temporal asymmetries in auditory perception. Hear. Res. *167*, 192–205.
33. Engineer, C.T., Perez, C.A., Chen, Y.H., Carraway, R.S., Reed, A.C., Shetake, J.A., Jakkamsetti, V., Chang, K.Q., and Kilgard, M.P. (2008). Cortical activity patterns predict speech discrimination ability. Nat. Neurosci. *11*, 603–608.
34. Gleichmann, M., Zhang, Y., Wood, W.H., 3rd, Becker, K.G., Mughal, M.R., Pazin, M.J., van Praag, H., Kobilo, T., Zonderman, A.B., Troncoso, J.C., et al. (2012). Molecular changes in brain aging and Alzheimer's disease are mirrored in experimentally silenced cortical neuron networks. Neurobiol. Aging *33*, e1–e18.
35. Martin del Campo, H.N., Measor, K.R., and Razak, K.A. (2012). Parvalbumin immunoreactivity in the auditory cortex of a mouse model of presbycusis. Hear. Res. *294*, 31–39.
36. Ouda, L., Druga, R., and Syka, J. (2008). Changes in parvalbumin immunoreactivity with aging in the central auditory system of the rat. Exp. Gerontol. *43*, 782–789.
37. Stanley, E.M., Fadel, J.R., and Mott, D.D. (2012). Interneuron loss reduces dendritic inhibition and GABA release in hippocampus of aged rats. Neurobiol. Aging *33*, e1–e13.
38. Scholl, B., Gao, X., and Wehr, M. (2010). Nonoverlapping sets of synapses drive on responses and off responses in auditory cortex. Neuron *65*, 412–421.
39. Lee, Y., López, D.E., Meloni, E.G., and Davis, M. (1996). A primary acoustic startle pathway: obligatory role of cochlear root neurons and the nucleus reticularis pontis caudalis. J. Neurosci. *16*, 3775–3789.
40. Li, L., Du, Y., Li, N., Wu, X., and Wu, Y. (2009). Top-down modulation of prepulse inhibition of the startle reflex in humans and rats. Neurosci. Biobehav. Rev. *33*, 1157–1167.
41. Dean, I., Robinson, B.L., Harper, N.S., and McAlpine, D. (2008). Rapid neural adaptation to sound level statistics. J. Neurosci. *28*, 6430–6438.
42. Scholl, B., Gao, X., and Wehr, M. (2008). Level dependence of contextual modulation in auditory cortex. J. Neurophysiol. *99*, 1616–1627.
43. Ulanovsky, N., Las, L., Farkas, D., and Nelken, I. (2004). Multiple time scales of adaptation in auditory cortex neurons. J. Neurosci. *24*, 10440–10453.
44. Wehr, M., and Zador, A.M. (2005). Synaptic mechanisms of forward suppression in rat auditory cortex. Neuron *47*, 437–445.
45. Atencio, C.A., and Schreiner, C.E. (2008). Spectrotemporal processing differences between auditory cortical fast-spiking and regular-spiking neurons. J. Neurosci. *28*, 3897–3910.
46. Ison, J.R., Allen, P.D., and O'Neill, W.E. (2007). Age-related hearing loss in C57BL/6J mice has both frequency-specific and non-frequency-specific components that produce a hyperacusis-like exaggeration of the acoustic startle reflex. J. Assoc. Res. Otolaryngol. *8*, 539–550.
47. Zar, J.H. (2010). Biostatistical Analysis, Fifth Edition (Upper Saddle River: Prentice-Hall).